ORGANOMETALLICS

pubs.acs.org/Organometallics

Article

Structural and Electronic Studies of Substituted *m*-Terphenyl Group 12 Complexes

Andrew J. Valentine, Laurence J. Taylor, Ana M. Geer, Cameron D. Huke, Katherine E. Wood, Will Tovey, William Lewis, Stephen P. Argent, Andrew M. Teale, Jonathan McMaster,* and Deborah L. Kays*

Cite This: *Organometallics* 2022, 41, 1426−1433

Read Online

ACCESS | Metrics & More | Article Recommendations | Supporting Information

ABSTRACT: The effects of *para*-substitution on the structural and electronic properties of four series of two-coordinate *m*-terphenyl Group 12 complexes $(R\text{-}Ar^{\#})_2M$ (M = Zn, Cd, Hg; R = *t*-Bu **1−3**, $SiMe_3$ **4−6**, Cl **7−9**, CF_3 **10−12**, where $R\text{-}Ar^{\#}$ = 2,6-{2,6-Xyl}$_2$-4-R-C_6H_2 and 2,6-Xyl = 2,6-$Me_2C_6H_3$) have been investigated. X-ray crystallography shows little structural variation across the series, with no significant change in the C−M−C bond distances and angles. However, considerable electronic differences are revealed by heteronuclear nuclear magnetic resonance (NMR) spectroscopy; a linear correlation is observed between the ^{113}Cd, ^{199}Hg, and ^{1}H (2,6-Xyl methyl protons) NMR chemical shifts of the *para*-substituted complexes and the Hammett constants for the R-substituents. Specifically, an upfield shift in the NMR signal is observed with increasingly electron-withdrawing R-substituents. Density functional theory (DFT) calculations are employed to attempt to rationalize these trends.

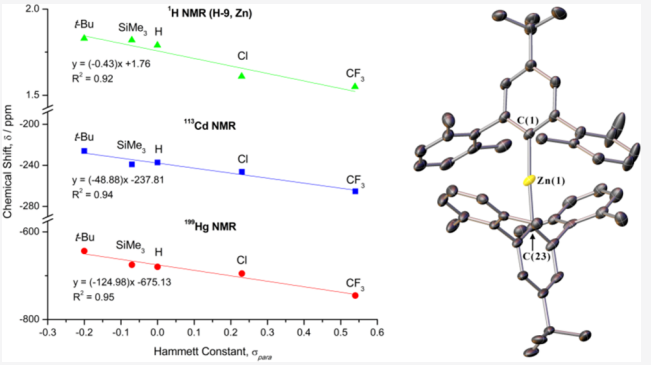

1. INTRODUCTION

The stabilization of low-coordinate Group 12 metal complexes exhibiting novel bonding modes and geometries has been explored through the use of sterically demanding ligands.[1−6] In contrast to the earliest examples of zinc, cadmium, and mercury dialkyl and diaryl complexes,[7−10] which incorporate necessary secondary stabilizing interactions, the bulky *m*-terphenyl framework[11,12] has enabled the isolation of strictly two-coordinate Group 12 systems such as $(2,6\text{-}Mes_2C_6H_3)_2Zn$ (Mes = 2,4,6-$Me_3C_6H_2$).[13,14] Other reports include the synthesis of a homologous series of Group 12 M−M-bonded species $(2,6\text{-}Dipp_2C_6H_3)_2M_2$ (M = Zn, Cd, Hg; Dipp = 2,6-*i*-$Pr_2C_6H_3$)[15,16] and the formation of a Zn−Zr−Zn unit in $[(2,6\text{-}Tripp_2C_6H_3)Zn]_2Zr(\eta^5\text{-}C_5H_5)_2$ (Tripp = 2,4,6-*i*-$Pr_3C_6H_2$).[17,18]

The application of Group 12 organometallic complexes in catalysis has rendered them invaluable reagents for synthesis. Organozinc compounds, for example, have proven useful in organic transformations,[19,20] alkali-metal-mediated zincation reactions,[21,22] and copolymerization reactions.[23,24] Organocadmium complexes, on the other hand, play a key role as molecular precursors in the synthesis of photoluminescent quantum dots,[25,26] while organomercurials feature prominently as ligand transmetallation reagents.[27,28]

Previous work within our group has explored the structural role of the *m*-terphenyl ligand upon three series of two-coordinate Group 12 diaryls $(2,6\text{-}Ar_2C_6H_3)_2M$ (M = Zn, Cd, Hg; Ar = 2,6-Xyl {2,6-$Me_2C_6H_3$}, 3,5-Xyl {3,5-$Me_2C_6H_3$}, Pmp {Me_5C_6}), where subtle changes in the steric pocket around the metal center were studied.[29] Thus, the bulkier 2,6-Xyl and Pmp flanking groups led to near-linear C−M−C bond angles [175.78(12)−180.0(0)°], whereas the less sterically hindered 3,5-Xyl group resulted in greater deviations from linearity [171.18(5)−176.4(2)°]. However, the effects of varying the electronic structure of the *m*-terphenyl ligand upon these Group 12 compounds have yet to be investigated.

Multiple studies by Power et al. have analyzed the electronic properties of metal complexes incorporating *para*-substituted *m*-terphenyl ligands.[30−32] One example is the quintuply-bonded arylchromium dimer, where a set of *para*-functionalized analogues $[(2,6\text{-}Dipp_2\text{-}4\text{-}R\text{-}C_6H_2)Cr]_2$ (R = H, $SiMe_3$, OMe, F) were prepared to probe the nature of the Cr−Cr bond.[33] Additional reports include the study of a series of *para*-substituted Group 14 complexes $(2,6\text{-}Mes_2\text{-}4\text{-}R\text{-}C_6H_2)_2M$ (M = Ge, Sn, Pb; R = H, $SiMe_3$, Cl)[34,35] and the analysis of the

Received: March 30, 2022
Published: May 30, 2022

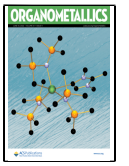

functionalized tin hydrides $[(2,6\text{-}Dipp_2\text{-}4\text{-}R\text{-}C_6H_2)Sn(\mu\text{-}H)]_2$ (R = H, $SiMe_3$, OMe, *t*-Bu).[36]

We have employed a series of *para*-substituted *m*-terphenyl ligands to study the role of electronic effects on the structures, bonding, and electronic properties of their Group 12 diaryl complexes. The diamagnetic nature of these Group 12 metal(II) species means that their electronic structures may be probed by NMR spectroscopy, which has been used previously to differentiate between *syn*- and *anti*-conformers in a series of naphthyl-substituted complexes $(2,6\text{-}Naph_2C_6H_3)_2M$ (M = Zn, $Cd{\cdot}OEt_2$, $Hg{\cdot}OEt_2$; Naph = 1-$C_{10}H_7$).[37] Herein, four series of novel *para*-substituted, two-coordinate, *m*-terphenyl Group 12 diaryls $(R\text{-}Ar^{\#})_2M$ ($R\text{-}Ar^{\#}$ = $2,6\text{-}\{2,6\text{-}Xyl\}_2\text{-}4\text{-}R\text{-}C_6H_2$; M = Zn, Cd, Hg; R = *t*-Bu, $SiMe_3$, Cl, CF_3) are reported and discussed alongside their unsubstituted analogues $(H\text{-}Ar^{\#})_2M$.[29] The geometric and electronic properties of these compounds are elucidated through X-ray crystallographic and NMR spectroscopic studies, respectively. We employ ^{113}Cd and ^{199}Hg NMR spectroscopies to assess the impact of the variation of the electronic structure of the ligand directly at the metal center.

2. RESULTS AND DISCUSSION

2.1. Synthesis. The reaction between the lithium complexes $[R\text{-}Ar^{\#}\text{-}Li]_2$ ($R\text{-}Ar^{\#}$ = $2,6\text{-}\{2,6\text{-}Xyl\}_2\text{-}4\text{-}R\text{-}C_6H_2$; R = *t*-Bu, $SiMe_3$, Cl, CF_3)[38] with one equivalent of $ZnCl_2$, $CdCl_2$, or $HgBr_2$ in a toluene/THF (10:1) mixture at room temperature yielded the Group 12 diaryl species $(t\text{-}Bu\text{-}Ar^{\#})_2M$ (M = Zn **1**, Cd **2**, Hg **3**), $(Me_3Si\text{-}Ar^{\#})_2M$ (M = Zn **4**, Cd **5**, Hg **6**), $(Cl\text{-}Ar^{\#})_2M$ (M = Zn **7**, Cd **8**, Hg **9**), and $(F_3C\text{-}Ar^{\#})_2M$ (M = Zn **10**, Cd **11**, Hg **12**) according to Scheme 1. Complexes **1**−**12** were recrystallized from a −30 °C *iso*-hexane solution to give colorless crystals in low-to-moderate isolated yields. Characterizations of **1**−**12** have been achieved by single-crystal X-ray diffraction, multinuclear (^1H, $^{13}C\{^1H\}$, $^{19}F\{^1H\}$, $^{29}Si\{^1H\}$, ^{113}Cd and ^{199}Hg) NMR spectroscopies, mass spectrometry, cyclic voltammetry (for **3** and **12**), and elemental analyses.

Scheme 1. Synthesis of Diaryl Complexes $(R\text{-}Ar^{\#})_2M$ (M = Zn, Cd, Hg; R = *t*-Bu 1−3, $SiMe_3$ 4−6, Cl 7−9, CF_3 10−12), where MX_2 Is $ZnCl_2$, $CdCl_2$, or $HgBr_2$[a]

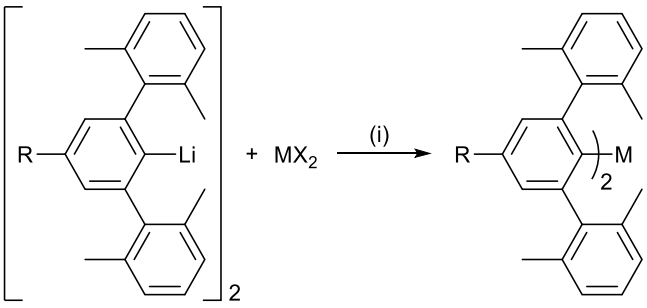

[a]Reaction conditions: (i) toluene/THF (10:1), room temperature, 16 h, −2 LiX.

2.2. Solid-State Characterization. The crystal structures of **1**−**12** confirm that all complexes are monomeric in the solid state, owing to the steric demands of the *m*-terphenyl ligands, with no intermolecular interactions between the metal centers. In all cases, the complexes are two-coordinate and quasi-linear, featuring a single metal center coordinated by two σ-bonded *m*-terphenyl ligands. Unlike the 3,5-Xyl complexes $[2,6\text{-}\{3,5\text{-}Xyl\}_2C_6H_3]_2M$ (M = Zn, Cd, Hg), no M···H contacts are formed to the flanking aryl rings.[29] The crystal structure of **1** is presented in Figure 1, with key measurements about the metal

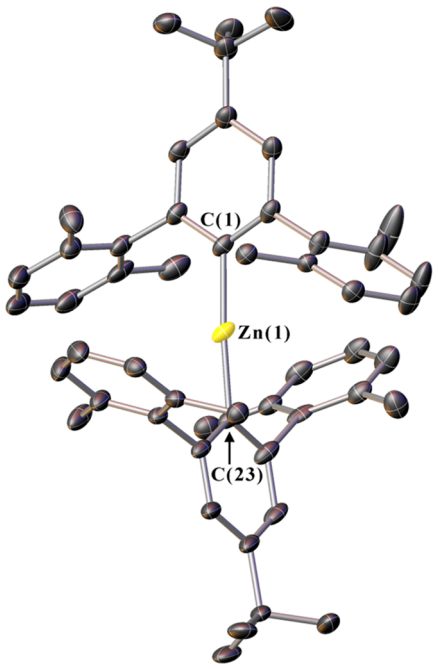

Figure 1. Crystal structure of **1**. Ellipsoids set at 30% probability. Disordered solvent and hydrogen atoms are omitted for clarity.

center for **1**−**12** provided in Table 1. Full crystallographic data for **1**−**12** are provided in Supporting Information Figures S40−S43 and Table S1 (M = Zn), Table S2 (M = Cd), and Table S3 (M = Hg). It should be noted that the crystal data for **4** are of low quality due to weak diffraction from a small crystal. Despite repeated attempts, it was not possible to grow high-quality crystals of **4**. However, the data are sufficient to demonstrate the connectivity of the molecule and are included here for completeness.

For each Group 12 metal, the corresponding series of *para*-substituted complexes show no significant change in the M−C bond distances as the functional group is varied. The Zn−C bond distances for **1**, **4**, **7**, and **10** fall within a narrow range [1.934(2)−1.953(12) Å] and are comparable to the previously reported unsubstituted analogue $(H\text{-}Ar^{\#})_2Zn$ [Zn(1)−C(1) = 1.949(4) Å, Zn(1)−C(23) = 1.944(4) Å].[29] These values also correlate with other zinc diaryl complexes in the literature, whose Zn−C bond distances range between 1.93 and 1.95 Å.[39−41]

A narrow range of M−C bond distances is also observed for **2**, **5**, **8**, and **11** [Cd−C = 2.098(14)−2.1215(16) Å] and for **3**, **6**, **9**, and **12** [Hg−C = 2.056(10)−2.098(3) Å], which mirror those of the unsubstituted analogues $(H\text{-}Ar^{\#})_2M$ (M = Cd, Hg) [Cd(1)−C(1) = 2.115(5) Å, Cd(1)−C(23) = 2.228(5) Å and Hg(1)−C(1) = 2.087(6) Å, Hg(1)−C(23) = 2.101(5) Å].[29] These values are comparable to other cadmium and mercury diaryl complexes, whose M−C bond distances range between 2.11−2.12 and 2.07−2.15 Å, respectively.[10,42−46] The reduction in M−C bond distance on moving from Cd to Hg can be attributed to a combination of relativistic effects and lanthanide contraction.[47−49]

https://doi.org/10.1021/acs.organomet.2c00156
Organometallics 2022, 41, 1426−1433

Table 1. Selected Bond Lengths (Å) and Angles (deg) for 1−12

compound	M	R	M(1)−C(1)	M(1)−C(23)	C(1)−M1−C(23)
1	Zn	*t*-Bu	1.937(2)	1.934(2)	175.87(10)
2	Cd	*t*-Bu	2.110(2)	2.110(2)	176.57(7)
3[a]	Hg	*t*-Bu	2.070(3)		175.91(13)
4[b]	Zn	$SiMe_3$	1.953(12)	1.951(13)	176.4(6)
5	Cd	$SiMe_3$	2.111(14)	2.098(14)	177.5(6)
6	Hg	$SiMe_3$	2.056(10)	2.063(10)	177.1(4)
7[c]	Zn	Cl	1.9418(17) [1.9429(17)]	1.9465(17) [1.9367(17)]	176.10(8) [176.84(9)]
8	Cd	Cl	2.120(2)	2.116(2)	177.42(10)
9	Hg	Cl	2.086(3)	2.085(3)	177.51(14)
10	Zn	CF_3	1.9449(13)	1.9483(13)	178.87(6)
11	Cd	CF_3	2.1159(16)	2.1215(16)	179.16(6)
12	Hg	CF_3	2.089(3)	2.098(3)	179.28(12)

[a]For **3**, C(1) = C(23) due to symmetry (Z' = 0.5). [b]Crystal data for **4** are of low quality due to weak diffraction from a very small crystal. Data are included here for completeness. [c]Measurements for the second molecule in asymmetric unit given in square brackets.

The C−M−C angles for **1**−**12** also present a reasonably narrow range of values. Thus, the C−Zn−C angles of **1**, **4**, **7**, and **10** [175.87(10)−178.87(6)°] are comparable to the C−Cd−C angles of **2**, **5**, **8**, and **11** [176.57(7)−179.16(6)°] and to the C−Hg−C angles of **3**, **6**, **9**, and **12** [175.91(13)−179.28(12)°], indicating little variation as the metal is changed. These values correlate with the C−M−C angles reported for the unsubstituted analogues $(H\text{-}Ar^{\#})_2M$ (M = Zn, Cd, Hg) [177.1(2)−179.9(3)°] but differ from the angles observed in the (less sterically hindered) 3,5-Xyl complexes $(3,5\text{-}Xyl_2C_6H_3)_2M$ (M = Zn, Cd, Hg) [171.18(5)−176.4(2)°].[29] The C−M−C angles for **1**−**12** are also similar to those of Mes_2M (M = Zn, Cd, Hg).[9,10]

In summary, the crystal structures of **1**−**12** show little structural variation as the *para*-substituent of the *m*-terphenyl ligand is varied. This suggests that the geometries of these complexes are dominated by steric and crystal packing effects, rather than the electronic structure of the ligand.

2.3. Solution-State Characterization. The electronic structures of **1**−**12** were studied by ^1H, $^{13}C\{^1H\}$, ^{113}Cd, and ^{199}Hg NMR spectroscopies in d_6-benzene and compared to those of the unsubstituted analogues $(H\text{-}Ar^{\#})_2M$ (M = Zn, Cd, Hg).[29] Here, a numbering scheme has been assigned to the *m*-terphenyl unit, as shown in Figure 2. The electronic strengths

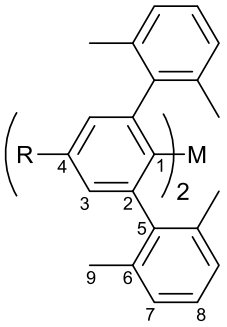

Figure 2. NMR numbering scheme for *m*-terphenyl complexes **1**−**12**.

of different *para*-substituents are quantified using Hammett constants, σ_{para}.[50] A comparison of the ^1H NMR spectra for complexes **1**−**12** reveals three noteworthy features (Table 2). First, the *meta*-protons (H-3) on the central aryl rings exhibit notable peak shifts as the *para*-substituent is changed, although no overall trend is evident. There is, however, a clear downfield shift in H-3 when varying the metal from Zn (6.76−7.14 ppm) to Cd (6.87−7.22 ppm) to Hg (6.92−7.30 ppm). Second, the 2,6-Xyl aryl protons (H-7 and H-8) for **1**−**12** remain relatively unshifted by changing the *para*-substituent or the metal, suggesting there is minimal electronic communication with the flanking aryl rings. Third, the 2,6-Xyl methyl protons (H-9) shift upfield with increased electron-withdrawing strength of the *para*-substituent. A plot of the chemical shifts, δ, against the Hammett constants, σ_{para}, reveals a linear correlation (Figures 3 and S1).[50] A similar trend was observed in recent studies of the analogous lithium complexes $[R\text{-}Ar^{\#}\text{-}Li]_2$ (R = *t*-Bu, $SiMe_3$, H, Cl, CF_3).[38] We note that the chemical shifts for H-9 are largely unaffected by the identity of the metal (Table 2).

The $^{13}C\{^1H\}$ NMR spectra of **1**−**12** show nine peaks for the carbons of the ligand framework, as well as additional peaks for the C-atoms of the *t*-Bu, $SiMe_3$, and CF_3 groups. A comparison of the spectra reveals that C-5 (143.2−147.4 ppm), C-6 (135.8−136.4 ppm), C-7 (127.8−128.3 ppm), C-8 (127.1−127.9 ppm), and C-9 (21.2−22.0 ppm) of the 2,6-Xyl groups remain relatively unshifted, irrespective of the nature of the metal or *para*-group (Table 2). This can again be attributed to poor electronic communication between the central and flanking aryl rings. However, the $^{13}C\{^1H\}$ NMR signals for the central aryl ring shift considerably with the notable exception of C-2 (Table 2). We note that the largest shifts are for the *ipso*-carbon atoms (C-1) where, in addition to a downfield shift in δ_C with increasing σ_{para} of the substituent, large downfield shifts of ca. 10 ppm are observed as the metal varies from Zn (148.5−156.8 ppm) to Cd (158.3−167.0 ppm) to Hg (169.1−176.0 ppm). For similar complexes in the literature, this downfield trend has been ascribed to the increasing Pauling electronegativity as Group 12 is descended (1.65, 1.69, and 2.00 for Zn, Cd, and Hg, respectively).[10,16,29,46,51−53]

The ^{113}Cd and ^{199}Hg NMR spectra of **2**, **5**, **8**, **11** and **3**, **6**, **9**, **12** were also recorded. Multiple NMR measurements revealed no change in chemical shift with varying analyte concentration, most likely due to the steric bulk of the ligands preventing interaction of the metal with the surrounding solvent.[54−56] In all cases, the ^{113}Cd and ^{199}Hg NMR spectra show a single peak indicating one metal environment in solution, in the same region as other literature metal diaryl complexes (see Table 3).[37,57−59] In previous work on the Group 12 diaryls $(2,6\text{-}Ar_2C_6H_3)_2M$ (M = Cd, Hg; Ar = 2,6-Xyl, 3,5-Xyl, Pmp),

https://doi.org/10.1021/acs.organomet.2c00156
Organometallics 2022, 41, 1426−1433

Table 2. Relevant ^{1}H and ^{13}C{^{1}H} NMR Chemical Shifts, δ, for the Metal Diaryls (R-Ar$^{\#}$)$_2$M (1−12, plus R = H)[29] [a]

			^{1}H and ^{13}C{^{1}H} NMR chemical shifts, δ (ppm)						
	(R-Ar$^{\#}$)$_2$M	R group	H-3	H-9	C-1	C-2	C-3	C-4	C-9
M = Zn	**1**	*t*-Bu	6.93	1.83	148.5	149.8	122.4	151.9	21.9
	4	$SiMe_3$	7.14	1.82	152.8	149.3	130.2	140.7	22.0
	lit.[b]	H	6.76	1.79	152.0	150.0	125.5	128.9	21.8
	7	Cl	6.78	1.61	150.2	151.6	125.7	135.4	21.6
	10	CF_3	7.05	1.55	156.8	150.7	122.1	131.5	21.6
M = Cd	**2**	*t*-Bu	7.02	1.84	158.3	149.4	122.0	151.4	21.5
	5	$SiMe_3$	7.22	1.82	162.9	149.1	129.7	140.0	21.6
	lit.[b]	H	6.87	1.80	161.9	149.6	125.1	128.4	21.5
	8	Cl	6.88	1.63	160.1	151.1	125.4	134.8	21.2
	11	CF_3	7.14	1.56	167.0	150.2	121.7	131.1	21.3
M = Hg	**3**	*t*-Bu	7.09	1.83	169.1	148.4	123.7	151.4	21.5
	6	$SiMe_3$	7.30	1.81	173.0	148.1	131.5	140.2	21.5
	lit.[b]	H	6.92	1.78	172.0	148.7	126.8	128.4	21.4
	9	Cl	6.92	1.61	170.2	150.1	127.0	134.7	21.2
	12	CF_3	7.20	1.54	176.0	149.3	123.6	131.1	21.2

[a]The flanking aryl atoms remain unshifted and thus have been omitted. [b]Literature NMR data for the unsubstituted complexes (H-Ar$^{\#}$)$_2$M (M = Zn, Cd, Hg), original data re-referenced to C_6D_6.[29]

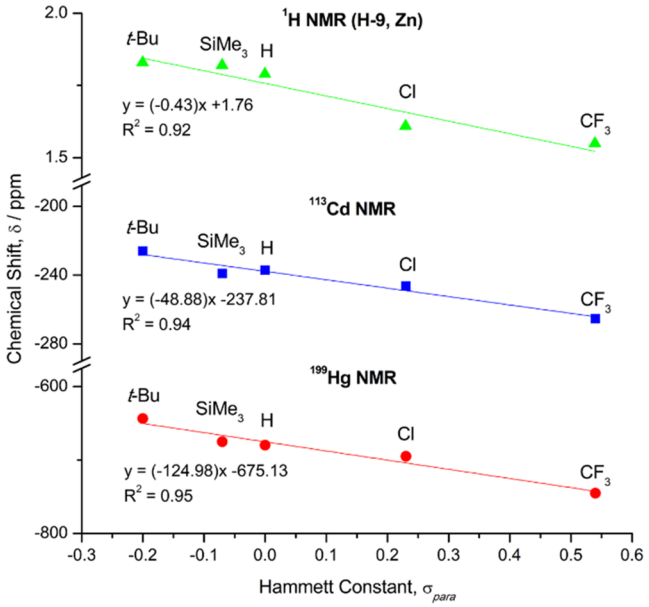

Figure 3. Plot of the ^{1}H (for flanking methyl protons, H-9), ^{113}Cd, and ^{199}Hg NMR chemical shifts, δ, for the metal diaryls (R-Ar$^{\#}$)$_2$M (**1**−**12**, plus R = H)[29] vs their Hammett constants, σ_{para}.[50] For clarity, the ^{1}H NMR (H-9) trend is given only for the Zn series; plots for the Cd and Hg series are provided in Supporting Information Figure S1.

increasing the steric bulk of the flanking groups was found to cause an upfield shift in their ^{113}Cd and ^{199}Hg NMR spectra.[29] However, since complexes **1**−**12** all feature the same flanking groups (2,6-Xyl) and are crystallographically similar, we suggest that steric effects are unlikely to have a major influence on their ^{113}Cd and ^{199}Hg NMR shifts.

A plot of the ^{113}Cd and ^{199}Hg NMR chemical shifts (δ) for each of the *para*-substituted complexes, vs their corresponding Hammett constant (σ_{para}) is shown in Figure 3.[50] Linear correlations can be fitted to the ^{113}Cd (blue line; R^2 = 0.96) and ^{199}Hg (red line; R^2 = 0.95) NMR data, both with a negative gradient, indicating that more electron-withdrawing substituents shift the NMR peak of the Cd and Hg centers further upfield. This trend is somewhat counterintuitive, as

Table 3. ^{113}Cd and ^{199}Hg NMR Chemical Shifts, δ, for the Metal Diaryls (R-Ar$^{\#}$)$_2$M (M = Cd, Hg; R = *t*-Bu 2−3, $SiMe_3$ 5−6, H,[29] Cl 8−9, CF_3 11−12)[50]

				NMR chemical shifts, δ (ppm)	
	(R-Ar$^{\#}$)$_2$M	R group	Hammett constant, σ_{para}	^{113}Cd	^{199}Hg
M = Cd, Hg	**2**, **3**	*t*-Bu	−0.20	−225.89	−642.81
	5, **6**	$SiMe_3$	−0.07	−239.07	−674.91
	lit.[a]	H	0.00	−239.36	−679.77
	8, **9**	Cl	0.23	−246.03	−695.04
	11, **12**	CF_3	0.54	−265.21	−745.00

[a]Literature NMR data for the unsubstituted complexes (H-Ar)$_2$M (M = Cd, Hg).[29,50]

electron-withdrawing groups might be expected to deshield the nuclei and cause a downfield shift. However, similar findings were reported for a series of *para*-substituted mercury diaryls (4-R-C_6H_4)$_2$Hg (R = OMe, Me, H, F, Cl, CF_3),[60−62] suggesting that these chemical shifts depend on more than simple σ donor effects. One hypothesis suggests that the bonding in organomercury compounds mainly involves the valence 6s orbital[63,64] since the 6p orbital is too high in energy to overlap. However, by incorporating electron-donating groups onto the ligand, the ligand orbitals increase in energy and overlap better with the 6p orbitals.[58,65] This populates the more diffuse 6p orbitals and depopulates the less diffuse 6s. Hence, the electron density around the metal center moves away from the nucleus and becomes more diffuse, resulting in less shielding and a downfield NMR shift.[58]

Cyclic voltammetry studies were also carried out on the mercury complexes **3** and **12** (R = *t*-Bu and CF_3) in THF solution (Supporting Information, Section S4). However, no redox events were observed upon scanning from −0.5 to −2.5 V (vs Fc^+/Fc) in either case (Figure S44), suggesting a large HOMO−LUMO gap for these complexes.

2.4. Computational Analysis. Density functional theory (DFT) calculations were employed to attempt to rationalize the trends in the NMR spectroscopic parameters. Full geometry optimizations (BP86/TZVP, see Supporting In-

https://doi.org/10.1021/acs.organomet.2c00156
Organometallics 2022, 41, 1426−1433

formation Section S5.1 for full details) were performed on **1**−**12**, as well as the unsubstituted analogues. All optimized structures displayed near-linear bond angles in a very narrow range (Table S5), although structures with M = Zn showed slightly greater distortion from linearity (C−Zn−C = 178.18−178.88°; C−Cd−C = 179.08−179.90°; C−Hg−C = 179.57−179.88°). Single-point calculations (PBE0/TZVP, see Supporting Information Section S5.2 for full details) were then performed on the optimized structures to obtain an estimate of the orbital energies. This showed that the HOMO energies, LUMO energies, and HOMO−LUMO gap all show negative correlation with σ_{para} (Figures S45−S47). The predicted HOMO−LUMO gap (5.1−5.6 eV) is large enough to account for the observed lack of redox events over the potential range −0.5 to −2.5 V vs Fc^+/Fc in the electrochemical experiments (see above).

A Quantum Theory of Atoms in Molecules (QTAIM) analysis was also employed on the optimized structures of (2,6-$Xyl_2C_6H_3)_2M$ (M = Zn, Cd, Hg; see Supporting Information Section S5.2 for details). This analysis did not locate any bond paths corresponding to C−H···M (M = Zn, Cd, Hg) agostic interactions, which might have accounted for the observed trend in the H-9 chemical shifts. This contrasts with the recently reported dimeric lithium complexes $[R\text{-}Ar^{\#}\text{-}Li]_2$ (R = *t*-Bu, $SiMe_3$, H, Cl, CF_3), where a trend in the ^1H NMR chemical shifts of equivalent protons was linked to C−H···Li agostic interactions.[38] However, for the Group 12 complexes, bond paths corresponding to C−H···C_{arene} interactions were observed between the H-9 protons and aromatic carbons of the flanking aryl rings situated opposite to them (Figure S48). Properties of the electron density at the bond critical points for these interactions are provided in Supporting Information Table S6.

Subsequently, the ^1H, ^{113}Cd, and ^{199}Hg NMR chemical shift parameters for **1**−**12** and the unsubstituted analogues were calculated using the ReSpect program.[66−71] These calculations were carried out on both the fully optimized structures used above, as well as the structures taken directly from the crystallographic data in which only the H atom positions had been optimized (see Supporting Information Section S5.1 for details). NMR shielding constants were calculated using the KT2 density functional approximation,[72] which was specifically designed for the calculation of NMR shielding constants. The calculations were carried out at two levels of theory: dyall-vdz[73,74] basis set for Zn/Cd/Hg and pcS-1[75] for all other atoms (vdz/pcS-1) or dyall-vtz[73] for Zn/Cd and pcS-2[75] for all other atoms (vtz/pcS-2). Calculations for the mercury complexes at the vtz/pcS-2 level could not be completed due to technical limitations of the ReSpect program.[66−71]

A summary of the calculated ^1H, ^{113}Cd, and ^{119}Hg NMR chemical shifts for the H-9 protons of **1**−**12** (in both the fully optimized and H-atom optimized geometries) are provided in Supporting Information Tables S9 and S10. Plots of the computed vs experimental shifts are shown in Supporting Information Figures S49−S56. In these, a weak positive correlation is observed between calculated and experimental shifts for the H-9 protons of all complexes (Figures S49−S53). This trend is evident in both the fully optimized and H-atom optimized structures and at both the vdz/pcS-1 and vtz/pcS-2 levels. However, the correlation is not particularly strong, and some computed results [particularly $(H\text{-}Ar^{\#})_2Zn$] deviate significantly from the experimental values. The experimental trend in ^1H NMR shifts for the H-9 protons occurs over such a narrow chemical shift range (ca. 0.3 ppm) that the accuracy of the DFT calculations may not be sufficient to reliably reproduce this behavior. Despite the lack of C−H···M (M = Zn, Cd, Hg) close contacts, the H-9 chemical shifts feature large paramagnetic contributions to the shielding constant (Tables S7 and S8), much like the analogous lithium complexes $[R\text{-}Ar^{\#}\text{-}Li]_2$ (R = *t*-Bu, $SiMe_3$, H, Cl, CF_3).[38] It is known that when the paramagnetic components are dominant, density functional methods often fail to achieve high accuracy, as appears to be the case here.

The computed ^{113}Cd and ^{199}Hg NMR chemical shifts (vdz/pcS-1) show relatively poor agreement with the experimental values. While the ^{113}Cd NMR shifts for the H-atom optimized structures appear to roughly correlate with the experimental values (Figure S54), this correlation is lost in the fully geometry optimized structures. No convincing correlation is observed for the ^{199}Hg shifts in either geometry (Figure S56). In addition, the computed chemical shifts differ significantly (by >100 ppm) from the experimental shifts in all cases. At the vtz/pcS-2 level, the computed ^{113}Cd shifts follow a similar trend relative to the experimental shifts as at the vdz/pcS-1 level (Figure S55), but the absolute values of the computed chemical shifts are closer to the experimental values.

These results suggest that the computed chemical shifts are strongly dependent on geometry, with small changes in the coordination environment of the metal resulting in dramatic changes in the computed shift. We propose that to model the NMR properties of these complexes more accurately, it may be necessary to perform dynamics calculations and account for conformational flexibility.

3. CONCLUSIONS

Four series of *para*-substituted *m*-terphenyl Group 12 complexes $(R\text{-}Ar^{\#})_2M$ (M = Zn, Cd, Hg; R = *t*-Bu **1**−**3**, $SiMe_3$ **4**−**6**, Cl **7**−**9**, CF_3 **10**−**12**) have been reported. While negligible structural differences are observed by X-ray crystallography, NMR spectroscopic studies reveal considerable electronic differences within the ligand framework and at the metal center. A linear correlation of the ^{113}Cd and ^{199}Hg NMR chemical shifts is observed with the Hammett constants of the *para*-groups. Moreover, the flanking methyl protons, H-9, exhibit similar shifts in their ^1H NMR spectra. In all cases, an upfield shift is observed with increasingly electron-withdrawing substituents. DFT modeling suggests that the H-9 ^1H NMR chemical shifts, as well as the ^{113}Cd and ^{199}Hg chemical shifts, all feature large paramagnetic contributions to the shielding constants. As a result, the experimental trends could not be reproduced by our computational analysis.

■ ASSOCIATED CONTENT

Supporting Information

The Supporting Information is available free of charge at https://pubs.acs.org/doi/10.1021/acs.organomet.2c00156.

Full experimental details for the synthesis, characterization, and crystallographic data (PDF)

Coordinates (XYZ)

Accession Codes

CCDC 2163371−2163382 contain the supplementary crystallographic data for this paper. These data can be obtained free of charge via www.ccdc.cam.ac.uk/data_request/cif, or by emailing data_request@ccdc.cam.ac.uk, or by contacting The

https://doi.org/10.1021/acs.organomet.2c00156
Organometallics 2022, 41, 1426−1433

Cambridge Crystallographic Data Centre, 12 Union Road, Cambridge CB2 1EZ, UK; fax: +44 1223 336033.

AUTHOR INFORMATION

Corresponding Authors

Jonathan McMaster − *School of Chemistry, University of Nottingham, Nottingham NG7 2RD, U.K.;* orcid.org/0000-0003-0917-7454; Email: Jonathan.McMaster@nottingham.ac.uk

Deborah L. Kays − *School of Chemistry, University of Nottingham, Nottingham NG7 2RD, U.K.;* orcid.org/0000-0002-4616-6001; Email: Deborah.Kays@nottingham.ac.uk

Authors

Andrew J. Valentine − *School of Chemistry, University of Nottingham, Nottingham NG7 2RD, U.K.;* orcid.org/0000-0003-2448-8883

Laurence J. Taylor − *School of Chemistry, University of Nottingham, Nottingham NG7 2RD, U.K.;* orcid.org/0000-0002-4948-4267

Ana M. Geer − *Departamento de Química Inorgánica, Instituto de Síntesis Química y Catálisis Homogénea (ISQCH), CSIC Universidad de Zaragoza, 50009 Zaragoza, Spain;* orcid.org/0000-0003-1115-6759

Cameron D. Huke − *School of Chemistry, University of Nottingham, Nottingham NG7 2RD, U.K.*

Katherine E. Wood − *School of Chemistry, University of Nottingham, Nottingham NG7 2RD, U.K.*

Will Tovey − *School of Chemistry, University of Nottingham, Nottingham NG7 2RD, U.K.*

William Lewis − *School of Chemistry, The University of Sydney, Sydney, NSW 2006, Australia;* orcid.org/0000-0001-7103-6981

Stephen P. Argent − *School of Chemistry, University of Nottingham, Nottingham NG7 2RD, U.K.;* orcid.org/0000-0002-3461-9675

Andrew M. Teale − *School of Chemistry, University of Nottingham, Nottingham NG7 2RD, U.K.;* orcid.org/0000-0001-9617-1143

Complete contact information is available at: https://pubs.acs.org/10.1021/acs.organomet.2c00156

Notes

The authors declare no competing financial interest.

ACKNOWLEDGMENTS

The authors acknowledge the EPSRC [Grant Numbers EP/R004064/1 and EP/L015633/1]; the Leverhulme Trust [Grant Number RPG-2014-317]; the European Research Council under H2020/ERC Consolidator Grant "topDFT" [Grant Number 772259]; and the University of Nottingham for financial support of this research. They also thank the University of Nottingham Analytical Services Team for mass spectrometry and NMR spectroscopy measurements. They are also grateful for access to the University of Nottingham's Augusta High Performance Computing service. The authors also acknowledge the Microanalysis Service, London Metropolitan University, and the University of Nottingham Analytical Services Team for elemental analyses.

REFERENCES

(1) Bürger, H.; Sawodny, W.; Wannagat, U. Darstellung Und Schwinkungsspektren von Silylamiden Der Elemente Zink, Cadmium Und Quecksilber. *J. Organomet. Chem.* **1965**, *3*, 113−120.

(2) Schumann, H.; Gottfriedsen, J.; Girgsdies, F. Homoleptische Zinkamide: Der Übergang Zu Monomeren Molekülen. *Z. Anorg. Allg. Chem.* **1997**, *623*, 1881−1884.

(3) Rees, W. S.; Just, O.; Schumann, H.; Weimann, R. First Structural Characterization of a Zinc-Bis(Dialkylamide) Compound. *Polyhedron* **1998**, *17*, 1001−1004.

(4) Schumann, H.; Gottfriedsen, J.; Dechert, S.; Girgsdies, F. Homoleptische Amide von Zink, Cadmium Und Quecksilber. *Z. Anorg. Allg. Chem.* **2000**, *626*, 747−758.

(5) Just, O.; Gaul, D. A.; Rees, W. S. Low-Coordinate Volatile Group 12 Amides: Syntheses and Crystal Structure Determinations of Dimeric $\{M\{N[Si(CH_3)_2CH_2CH_2Si(CH_3)_2]\}_2\}_2$; M = Zn, Cd and Monomeric $Hg\{N[Si(CH_3)_2CH_2CH_2Si(CH_3)_2]\}_2$. *Polyhedron* **2001**, *20*, 815−821.

(6) Hicks, J.; Underhill, E. J.; Kefalidis, C. E.; Maron, L.; Jones, C. A Mixed-Valence Tri-Zinc Complex, [LZnZnZnL] (L = Bulky Amide), Bearing a Linear Chain of Two-Coordinate Zinc Atoms. *Angew. Chem., Int. Ed.* **2015**, *54*, 10000−10004.

(7) Markies, P. R.; Schat, G.; Akkerman, O. S.; Bickelhaupt, F.; Smeets, W. J. J.; Spek, A. L. Coordinational Behavior of Solvent-Free Diorganylzinc Compounds: The Remarkable X-Ray Structure of Dimeric Diphenylzinc. *Organometallics* **1990**, *9*, 2243−2247.

(8) Alsina, T.; Clegg, W.; Fraser, K. A.; Sola, J. Homoleptic Cyclohexanethiolato Complexes of Mercury(II). *J. Chem. Soc., Dalton Trans.* **1992**, 1393−1399.

(9) Cole, S. C.; Coles, M. P.; Hitchcock, P. B. Dimesitylzinc: A Strictly 2-Coordinate, Homoleptic Diarylzinc Compound. *Dalton Trans.* **2003**, 3663−3664.

(10) Hayashi, M.; Bolte, M.; Wagner, M.; Lerner, H.-W. Crystal Structures and Chemical Properties of Dimesitylcadmium and Dimesitylmercury. *Z. Anorg. Allg. Chem.* **2011**, *637*, 646−649.

(11) Clyburne, J. A. C.; McMullen, N. Unusual Structures of Main Group Organometallic Compounds Containing *m*-Terphenyl Ligands. *Coord. Chem. Rev.* **2000**, *210*, 73−99.

(12) Twamley, B.; Haubrich, S. T.; Power, P. P. Element Derivatives of Sterically Encumbering Terphenyl Ligands. In *Advances in Organometallic Chemistry*, West, R.; Hill, A. F., Eds.; Academic Press, 1999; Vol. *44*, pp 1−65.

(13) Niemeyer, M.; Power, P. P. Synthesis and Structure of the Solvent-Free Sodium Aryl $(NaC_6H_3\text{-}2,6\text{-}Mes_2)_2$. *Organometallics* **1997**, *16*, 3258−3260.

(14) Schröder, A.; Enno, L.; Beckmann, J. Synthesis and Structure of Bis(*m*-Terphenyl)Zinc $(2,6\text{-}Mes_2C_6H_3)_2Zn$. *Main Group Met. Chem.* **2014**, *37*, 155−157.

(15) Zhu, Z.; Wright, R. J.; Olmstead, M. M.; Rivard, E.; Brynda, M.; Power, P. P. A Zinc−Zinc-Bonded Compound and Its Derivatives Bridged by One or Two Hydrogen Atoms: A New Type of Zn−Zn Bonding. *Angew. Chem., Int. Ed.* **2006**, *45*, 5807−5810.

(16) Zhu, Z.; Brynda, M.; Wright, R. J.; Fischer, R. C.; Merrill, W. A.; Rivard, E.; Wolf, R.; Fettinger, J. C.; Olmstead, M. M.; Power, P. P. Synthesis and Characterization of the Homologous M−M Bonded Series Ar'MMAr' (M = Zn, Cd, or Hg; Ar' = $C_6H_3\text{-}2,6\text{-}(C_6H_3\text{-}2,6\text{-}Pr^i_2)_2$) and Related Arylmetal Halides and Hydride Species. *J. Am. Chem. Soc.* **2007**, *129*, 10847−10857.

(17) Wang, Y.; Quillian, B.; Wannere, C. S.; Wei, P.; Schleyer, P. vR.; Robinson, G. H. A Trimetallic Compound Containing Zn−Zr Bonds: $Cp_2Zr(ZnR)_2$ (Cp = C_5H_5; R = $C_6H_3\text{-}2,6\text{-}(2,4,6\text{-}i\text{-}Pr_3C_6H_2)_2$). *Organometallics* **2007**, *26*, 3054−3056.

(18) Kays, D. L. The Stabilisation of Organometallic Complexes Using *m*-Terphenyl Ligands. In *Organometallic Chemistry* Fairlamb, I. J. S.; Lynam, J. S., Eds.; Royal Society of Chemistry: Cambridge, 2010; Vol. *36*, pp 56−76.

(19) Negishi, E.; Zeng, X.; Tan, Z.; Qian, M.; Hu, Q.; Huang, Z. Metal-Catalyzed Cross-Coupling Reactions. In *Metal-Catalyzed Cross-*

Coupling Reactions de Meijere, A.; Diederich, F., Eds.; Wiley-VCH: Weinheim, Germany, 2004; p 815.
(20) *The Chemistry of Organozinc Compounds* Rappoport, Z.; Marek, I., Eds.; Wiley: Chichester, UK, 2006.
(21) Kennedy, A. R.; Klett, J.; Mulvey, R. E.; Wright, D. S. Synergic Sedation of Sensitive Anions: Alkali-Mediated Zincation of Cyclic Ethers and Ethene. *Science* **2009**, *326*, 706−708.
(22) Armstrong, D. R.; Clegg, W.; Dale, S. H.; Hevia, E.; Hogg, L. M.; Honeyman, G. W.; Mulvey, R. E. Directed *meta*-Metalation Using Alkali-Metal-Mediated Zincation. *Angew. Chem., Int. Ed.* **2006**, *45*, 3775−3778.
(23) Coates, G. W.; Moore, D. R. Discrete Metal-Based Catalysts for the Copolymerization of CO_2 and Epoxides: Discovery, Reactivity, Optimization, and Mechanism. *Angew. Chem., Int. Ed.* **2004**, *43*, 6618−6639.
(24) Sugimoto, H.; Inoue, S. Copolymerization of Carbon Dioxide and Epoxide. *J. Polym. Sci., A: Polym. Chem.* **2004**, *42*, 5561−5573.
(25) Boyle, T. J.; Bunge, S. D.; Alam, T. M.; Holland, G. P.; Headley, T. J.; Avilucea, G. Cadmium Amido Alkoxide and Alkoxide Precursors for the Synthesis of Nanocrystalline CdE (E = S, Se, Te). *Inorg. Chem.* **2005**, *44*, 1309−1318.
(26) Bochmann, M.; Webb, K.; Harman, M.; Hursthouse, M. B. Synthesis, Structure, and Gas-Phase Decomposition of $[Cd(EC_6H_2tBu_3)_2]_2$ (E = S, Se): First Examples of Low-Coordinate Volatile Cadmium Chalcogenolato Complexes. *Angew. Chem., Int. Ed.* **1990**, *29*, 638−639.
(27) Luo, B.; Gladfelter, W. L. Synthesis and Thermolysis of Alkyl- and Phenylamido Diphenylgallium, $[Ph_2GaN(H)R]_2$. Isolation and Structural Characterization of $(PhGaNMe)_7$ and $(PhGaNPh)_4$. *Inorg. Chem.* **2002**, *41*, 590−597.
(28) Castillo, I.; Tilley, T. D. Mechanistic Aspects of Samarium-Mediated σ-Bond Activations of Arene C−H and Arylsilane Si−C Bonds. *J. Am. Chem. Soc.* **2001**, *123*, 10526−10534.
(29) Blundell, T. J.; Hastings, F. R.; Gridley, B. M.; Moxey, G. J.; Lewis, W.; Blake, A. J.; Kays, D. L. Ligand Influences on Homoleptic Group 12 M-Terphenyl Complexes. *Dalton Trans.* **2014**, *43*, 14257−14264.
(30) Fischer, R. C.; Pu, L.; Fettinger, J. C.; Brynda, M. A.; Power, P. P. Very Large Changes in Bond Length and Bond Angle in a Heavy Group 14 Element Alkyne Analogue by Modification of a Remote Ligand Substituent. *J. Am. Chem. Soc.* **2006**, *128*, 11366−11367.
(31) Zhu, Z.; Fischer, R. C.; Ellis, B. D.; Rivard, E.; Merrill, W. A.; Olmstead, M. M.; Power, P. P.; Guo, J. D.; Nagase, S.; Pu, L. Synthesis, Characterization and Real Molecule DFT Calculations for Neutral Organogallium(I) Aryl Dimers and Monomers: Weakness of Gallium−Gallium Bonds in Digallenes and Digallynes. *Chem. − Eur. J.* **2009**, *15*, 5263−5272.
(32) Peng, Y.; Fischer, R. C.; Merrill, W. A.; Fischer, J.; Pu, L.; Ellis, B. D.; Fettinger, J. C.; Herber, R. H.; Power, P. P. Substituent Effects in Ditetrel Alkyne Analogues: Multiple vs. Single Bonded Isomers. *Chem. Sci.* **2010**, *1*, 461−468.
(33) Wolf, R.; Ni, C.; Nguyen, T.; Brynda, M.; Long, G. J.; Sutton, A. D.; Fischer, R. C.; Fettinger, J. C.; Hellman, M.; Pu, L.; Power, P. P. Substituent Effects in Formally Quintuple-Bonded ArCrCrAr Compounds (Ar = Terphenyl) and Related Species. *Inorg. Chem.* **2007**, *46*, 11277−11290.
(34) Wilfling, P.; Schittelkopf, K.; Flock, M.; Herber, R. H.; Power, P. P.; Fischer, R. C. Influence of Ligand Modifications on Structural and Spectroscopic Properties in Terphenyl Based Heavier Group 14 Carbene Homologues. *Organometallics* **2015**, *34*, 2222−2232.
(35) Simons, R. S.; Pu, L.; Olmstead, M. M.; Power, P. P. Synthesis and Characterization of the Monomeric Diaryls $M\{C_6H_3\text{-}2,6\text{-}Mes_2\}_2$ (M = Ge, Sn, or Pb; Mes = 2,4,6-$Me_3C_6H_2$−) and Dimeric Aryl−Metal Chlorides $[M(Cl)\{C_6H_3\text{-}2,6\text{-}Mes_2\}]_2$ (M = Ge or Sn). *Organometallics* **1997**, *16*, 1920−1925.
(36) Rivard, E.; Fischer, R. C.; Wolf, R.; Peng, Y.; Merrill, W. A.; Schley, N. D.; Zhu, Z.; Pu, L.; Fettinger, J. C.; Teat, S. J.; Nowik, I.; Herber, R. H.; Takagi, N.; Nagase, S.; Power, P. P. Isomeric Forms of Heavier Main Group Hydrides: Experimental and Theoretical Studies of the $[Sn(Ar)H]_2$ (Ar = Terphenyl) System. *J. Am. Chem. Soc.* **2007**, *129*, 16197−16208.
(37) Gridley, B. M.; Moxey, G. J.; Lewis, W.; Blake, A. J.; Kays, D. L. Conformational Isomerism in Monomeric, Low-Coordinate Group 12 Complexes Stabilized by a Naphthyl-Substituted *m*-Terphenyl Ligand. *Chem. − Eur. J.* **2013**, *19*, 11446−11453.
(38) Valentine, A. J.; Geer, A. M.; Taylor, L. J.; Teale, A. M.; Wood, K. E.; Williams, H. E. L.; Lewis, W.; Argent, S. P.; McMaster, J.; Kays, D. L. Structural and Electronic Studies of Substituted *m*-Terphenyl Lithium Complexes. *Dalton Trans.* **2021**, *50*, 722−728.
(39) Sun, Y.; Piers, W. E.; Parvez, M. The Solid-State Structure of Bis(Pentafluorophenyl)Zinc. *Can. J. Chem.* **1998**, *76*, 513−517.
(40) Chisholm, M. H.; Gallucci, J. C.; Yin, H.; Zhen, H. Arylzinc Alkoxides: $[ArZnOCHPr^i_2]_2$ and $Ar_2Zn_3(OCHPr^i_2)_4$ When Ar = C_6H_5, *p*-$CF_3C_6H_4$, 2,4,6-$Me_3C_6H_2$, and C_6F_5. *Inorg. Chem.* **2005**, *44*, 4777−4785.
(41) Westerhausen, M.; Oßberger, M. W.; Alexander, J. S.; Ruhlandt-Senge, K. Influence of the Steric Demand of the 2,4,6-Trialkylphenyl Substituents on the Structures and Reactivity of Diarylzinc. *Z. Anorg. Allg. Chem.* **2005**, *631*, 2836−2841.
(42) Braun, U.; Böck, B.; Nöth, H.; Schwab, I.; Schwartz, M.; Weber, S.; Wietelmann, U. Reactions of Group 13 and 14 Hydrides and Group 1, 2, 13 and 14 Organyl Compounds with (*tert*-Butylimino)-(2,2,6,6-Tetramethylpiperidino)Borane. *Eur. J. Inorg. Chem.* **2004**, *2004*, 3612−3628.
(43) Strasdeit, H.; Büsching, I.; Duhme, A.-K.; Pohl, S. Structure of the Two-Coordinate Cadmium Complex Bis(Pentafluorophenyl)-Cadmium(II), $[Cd(C_6F_5)_2]$. *Acta Crystallogr., Sect. C* **1993**, *49*, 576−578.
(44) Glidewell, C.; Low, J. N.; Wardell, J. L. Diphenylmercury, Redetermined at 120K: Sheets Built from a Single C—H···π(Arene) Hydrogen Bond. *Acta Crystallogr., Sect. C* **2005**, *61*, m107−m108.
(45) Huffman, J. C.; Nugent, W. A.; Kochi, J. K. Molecular Distortions in Sterically Congested Organometals. Crystal Structure of Bis(2,4,6-tri-*tert*-butylphenyl)mercury. *Inorg. Chem.* **1980**, *19*, 2749−2755.
(46) Brooker, S.; Bertel, N.; Stalke, D.; Noltemeyer, M.; Roesky, H. W.; Sheldrick, G. M.; Edelmann, F. T. Main-Group Chemistry of the 2,4,6-Tris(trifluoromethyl)phenyl Substituent: X-Ray Crystal Structures of $[2,4,6\text{-}(CF_3)_3C_6H_2]_2Zn$, $[2,4,6\text{-}(CF_3)_3C_6H_2]_2Cd(MeCN)$ and $[2,4,6\text{-}(CF_3)_3C_6H_3]_2Hg$. *Organometallics* **1992**, *11*, 192−195.
(47) Cordero, B.; Gómez, V.; Platero-Prats, A. E.; Revés, M.; Echeverría, J.; Cremades, E.; Barragán, F.; Alvarez, S. Covalent Radii Revisited. *Dalton Trans.* **2008**, 2832−2838.
(48) Ziegler, T.; Snijders, J. G.; Baerends, E. J. Relativistic Effects on Bonding. *J. Chem. Phys.* **1981**, *74*, 1271−1284.
(49) Pyykko, P. Relativistic Effects in Structural Chemistry. *Chem. Rev.* **1988**, *88*, 563−594.
(50) Hansch, C.; Leo, A.; Taft, R. W. A Survey of Hammett Substituent Constants and Resonance and Field Parameters. *Chem. Rev.* **1991**, *91*, 165−195.
(51) Allred, A. L. Electronegativity Values from Thermochemical Data. *J. Inorg. Nucl. Chem.* **1961**, *17*, 215−221.
(52) Heinekey, D. M.; Stobart, S. R. Aspects of Organocadmium Chemistry. 1. Bis[(Trimethylsilyl)methyl]Cadmium and Relationship with Homoleptic Zinc and Mercury Compounds. *Inorg. Chem.* **1978**, *17*, 1463−1466.
(53) Arnold, J.; Tilley, T. D.; Rheingold, A. L.; Geib, S. J. Preparation and Characterization of Tris(Trimethylsilyl)Silyl Derivatives of Zinc, Cadmium, and Mercury. X-Ray Crystal Structure of $Zn[Si(SiMe_3)_3]_2$. *Inorg. Chem.* **1987**, *26*, 2106−2109.
(54) Summers, M. F. ^{113}Cd NMR Spectroscopy of Coordination Compounds and Proteins. *Coord. Chem. Rev.* **1988**, *86*, 43−134.
(55) Munataka, M.; Kitagawa, S.; Yagi, F. Cadmium-113 NMR of Cadmium(II) Complexes with Ligands Containing N-Donor Atoms. Dependence of the Chemical Shift upon the Ligand Basicity, Chelate Ring Size, Counteranion, and Cadmium Concentration. *Inorg. Chem.* **1986**, *25*, 964−970.

https://doi.org/10.1021/acs.organomet.2c00156
Organometallics 2022, 41, 1426−1433

(56) Sens, M. A.; Wilson, N. K.; Ellis, P. D.; Odom, J. D. Mercury-199 Fourier Transform Nuclear Magnetic Resonance Spectroscopy. *J. Magn. Reson.* **1975**, *19*, 323−336.
(57) Cardin, A. D.; Ellis, P. D.; Odom, J. D.; Howard, J. W. Cadmium-113 Fourier Transform Nuclear Magnetic Resonance Spectroscopy. *J. Am. Chem. Soc.* **1975**, *97*, 1672−1679.
(58) Rowland, K. E.; Thomas, R. D. Carbon-13 and Mercury-199 NMR Data for Methyl-Substituted Bisaryl Mercury Compounds. *Magn. Reson. Chem.* **1985**, *23*, 916−919.
(59) Wrackmeyer, B.; Contreras, R. ^{199}Hg NMR Parameters. In *Annual Reports on NMR Spectroscopy*, Webb, G. A., Ed.; Academic Press, 1992; Vol. *24*, pp 267−329.
(60) Borzo, M.; Maciel, G. E. ^{199}Hg Chemical Shifts of Organomercury Compounds by Fourier Transform NMR. *J. Magn. Reson.* **1975**, *19*, 279−282.
(61) Wells, P. R.; Hawker, D. W. Mercury-199 NMR Chemical Shifts in Substituted Diphenylmercury and Phenylmercuric Chloride. *Org. Magn. Reson.* **1981**, *17*, 26−27.
(62) Craik, D. J. Substituent Effects on Nuclear Shielding. In *Annual Reports on NMR Spectroscopy*, Webb, G. A., Ed.; Academic Press, 1984; Vol. *15*, pp 91−92.
(63) DeKock, R. L.; Baerends, E. J.; Boerrigter, P. M.; Hengelmolen, R. Electronic Structure and Bonding of Dimethylmercury, Mercury(II) Cyanide, Methylmercury Cyanide, Bis(1-Propynyl)Mercury, and Methyl(Trimethylphosphine)Gold. *J. Am. Chem. Soc.* **1984**, *106*, 3387−3396.
(64) Nakatsuji, H.; Kanda, K.; Endo, K.; Yonezawa, T. Theoretical Study of the Metal Chemical Shift in Nuclear Magnetic Resonance. Silver, Cadmium, Copper, and Zinc Complexes. *J. Am. Chem. Soc.* **1984**, *106*, 4653−4660.
(65) Fedorov, L. A.; Faingor, B. A.; Golovchenko, L. S.; Kravtsov, D. N. Study of Organomercury Compounds by High-Resolution NMR. *J. Struct. Chem.* **1979**, *19*, 549−554.
(66) Repisky, M.; Komorovsky, S.; Malkin, V. G.; Malkina, O. L.; Kaupp, M.; Ruud, K.; Bast, R.; Di Remigio, R.; Ekström, U.; Kadek, M.; Knecht, S.; Konecny, L.; Malkin, E.; Ondik, I. M. *ReSpect 5.1.0, Relativistic Spectroscopy DFT Program; 5.1.0*, 2019. http://www.respectprogram.org.
(67) Komorovský, S.; Repiský, M.; Malkina, O. L.; Malkin, V. G.; Malkin Ondík, I.; Kaupp, M. A Fully Relativistic Method for Calculation of Nuclear Magnetic Shielding Tensors with a Restricted Magnetically Balanced Basis in the Framework of the Matrix Dirac−Kohn−Sham Equation. *J. Chem. Phys.* **2008**, *128*, No. 104101.
(68) Komorovský, S.; Repiský, M.; Malkina, O. L.; Malkin, V. G. Fully Relativistic Calculations of NMR Shielding Tensors Using Restricted Magnetically Balanced Basis and Gauge Including Atomic Orbitals. *J. Chem. Phys.* **2010**, *132*, No. 154101.
(69) Komorovsky, S.; Repisky, M.; Malkin, E.; Demissie, T. B.; Ruud, K. Four-Component Relativistic Density-Functional Theory Calculations of Nuclear Spin−Rotation Constants: Relativistic Effects in p-Block Hydrides. *J. Chem. Theory Comput.* **2015**, *11*, 3729−3739.
(70) Repisky, M.; Komorovsky, S.; Bast, R.; Ruud, K. Relativistic Calculations of Nuclear Magnetic Resonance Parameters. In *New Developments in NMR*, Jackowski, M. J. J., Ed.; The Royal Society of Chemistry, 2016; pp 267−303.
(71) Repiský, M.; Komorovský, S.; Malkina, O. L.; Malkin, V. G. Restricted Magnetically Balanced Basis Applied for Relativistic Calculations of Indirect Nuclear Spin−Spin Coupling Tensors in the Matrix Dirac−Kohn−Sham Framework. *Chem. Phys.* **2009**, *356*, 236−242.
(72) Keal, T. W.; Tozer, D. J. The Exchange-Correlation Potential in Kohn−Sham Nuclear Magnetic Resonance Shielding Calculations. *J. Chem. Phys.* **2003**, *119*, 3015−3024.
(73) Dyall, K. G. Relativistic Double-Zeta, Triple-Zeta, and Quadruple-Zeta Basis Sets for the 4d Elements Y-Cd. *Theor. Chem. Acc.* **2007**, *117*, 483−489.
(74) Dyall, K. G.; Gomes, A. S. P. Revised Relativistic Basis Sets for the 5d Elements Hf-Hg. *Theor. Chem. Acc.* **2010**, *125*, 97−100.
(75) Jensen, F. Basis Set Convergence of Nuclear Magnetic Shielding Constants Calculated by Density Functional Methods. *J. Chem. Theory Comput.* **2008**, *4*, 719−727.

https://doi.org/10.1021/acs.organomet.2c00156
Organometallics 2022, 41, 1426−1433